

Low energy chiral constants from epsilon-regime simulations with improved Wilson fermions

Anna Hasenfratz*

Department of Physics, University of Colorado, Boulder, Colorado-80309-390, USA

Roland Hoffmann†

Bergische Universität Wuppertal, Gausstraße 20, 42219 Wuppertal, Germany

Stefan Schaefer‡

*Institut für Physik, Humboldt Universität,
Newtonstraße 15, 12489 Berlin, Germany*

Abstract

We present a lattice QCD calculation of the low-energy constants of the leading order chiral Lagrangian. In these simulations the epsilon regime is reached by using tree-level improved nHYP Wilson fermions combined with reweighting in the quark mass. We analyze two point functions on two ensembles with lattices of size $(1.85\text{fm})^4$ and $(2.8\text{fm})^4$, and at several quark mass values between 4 and 20 MeV. The data are well fitted with next-to-leading order chiral perturbative formulas and predict $F = 90(4)\text{MeV}$ and $\Sigma^{1/3} = 248(6)\text{MeV}$ in the $\overline{\text{MS}}$ scheme at 2 GeV.

*Electronic address: anna@eotvos.colorado.edu

†Electronic address: hoffmann@pizero.colorado.edu

‡Electronic address: sschaef@physik.hu-berlin.de

I. INTRODUCTION

At low energies, quantum chromodynamics can be described by a low-energy effective theory, chiral perturbation theory[1], χ PT. To leading order, it has two *a priori* unknown parameters, the chiral condensate and the pion decay constant. In this paper, we compute these constants by an *ab initio* computation. Our strategy itself is not new: we compute two-point functions in the epsilon regime and fit them to their χ PT predictions. However, for chiral perturbation theory to be an accurate description of low-energy phenomena, we need calculations on the QCD side at very low pion masses, probably lower than typically reached in current simulations, and at the same time on large enough volumes to control higher order corrections.

Basically, there are two regions in parameter space where calculation of chiral perturbation theory can be carried out: one is the so-called p -regime where we are essentially at infinite volume. The pion wave length is much smaller than the size of the box, and the small corrections due to its finite extent can be taken into account analytically.

The other region is the ϵ -regime[2]. There the pion wave length is much larger than the spatial and temporal size of the lattice. One can carry out the integrals over the (effectively) constant pion modes exactly and arrive at a different power counting. This regime has considerable appeal. First of all, even at next-to-leading order, only the two leading order low-energy constants of chiral perturbation theory enter into observables[3, 4]. Second, being fundamentally a finite volume regime, once one has reached it, lowering the pion mass actually improves the validity of χ PT at a given order, whereas in the p -regime one needs to increase the volume at the same time.

The problem, however, lies in the task to actually reach this regime in numerical simulations. Because the epsilon expansion is in powers of $1/(FL)^2$, it turns out that we actually need a fairly big volume and therefore a very small quark mass to satisfy the condition $m_\pi \ll 1/L$. This poses many algorithmical problems. In a recent publication [5] we have presented a setup with which we can actually reach the regime of small quark masses at moderate cost avoiding many of the problems a more direct approach would face. We propose to use smeared link improved Wilson fermions [6, 7] to generate an ensemble of gauge configurations above the desired quark mass. From this ensemble, we reweight to the quark mass which we actually want to reach. Using this method, we manage to reduce the sea quark mass by roughly a factor of 2 to 4.

Reweighting has another advantage apart from the actual possibility to go to such light quarks. At very small quark mass statistical fluctuations grow dramatically because the mass no longer provides an infrared cutoff. Therefore, very small eigenvalues of the Dirac operator can appear, which are suppressed by the fermion determinant, but also lead to large values of the measured observables. We thus have an anticorrelation between the weight and the function value which means importance sampling breaks down. Reweighting avoids this problem. The small eigenvalues are not as efficiently suppressed, the region of large signal gets over-sampled and the error is actually reduced.

One might wonder how the explicit chiral symmetry breaking of Wilson fermions influence

simulations done with very light quarks in the epsilon regime. Unlike in the p -regime, the finite volume of the ϵ -regime provides the system with an effective, dynamical IR cut-off. The chiral symmetry violations will remain manageable even in the chiral limit as long as they are small compared to the inverse lattice size. The numerical study of the continuum limit to prove this expectation will be the subject of a future work.

In the current paper, we apply reweighting to a large volume data set and provide measurements of the low-energy constants F and Σ . We already mentioned that this type of simulation is not new. A number of quenched studies have been carried out [8, 9, 10, 11, 12, 13] using overlap fermions, which proved the feasibility of the method but also highlighted the need for sufficiently large volume. Recently, there also have been computations with dynamical overlap[14] and twisted mass[15] fermions to which we will compare our results in the conclusion. For a recent review of these calculations see Ref. [16]. The strength of our calculation is that we compare two different volumes, of which the larger one has not been reached in previous studies. The simulations in this work were fairly inexpensive, and it is within reach to repeat the calculation at a finer lattice spacing to verify scaling.

The outline of this paper is the following: We first describe in Sec. II the set-up of our simulations, the generation of the ensemble of gauge configurations and the details of our reweighting procedure. The relevant renormalization constants are computed in Sec. III using the RI-MOM scheme. In Sec. IV we collect the ϵ -regime formulas, the procedure of the extraction of the low-energy constants and give the results.

II. SIMULATIONS

The numerical simulations for this project were done with 2 flavors of nHYP smeared Wilson-clover fermions and one-loop Symanzik improved gauge action. The action and the simulation method are described in details in Refs. [6, 7]. We use tree-level $c_{SW} = 1.0$ clover coefficient, so our action is not fully $\mathcal{O}(a)$ improved. Based on our quenched investigation [17], we expect that a nonperturbatively improved action would require $c_{SW} \lesssim 1.2$, so even with only tree-level improvement the $\mathcal{O}(a)$ corrections are likely small. We have generated two sets of gauge ensembles, both at gauge coupling $\beta = 7.2$. The first set consists of 16^4 configurations at $\kappa = 0.1278$, the second 24^4 configurations at $\kappa = 0.12805$. We have 180 and 154 thermalized configurations, separated by 5 trajectories at the two volumes. The autocorrelation is 3-4 trajectories for the plaquette, and about the same for the two point functions. Preliminary results using the first set were already reported in Ref. [5].

We set the lattice scale from the static quark potential, using $r_0 = 0.49$ fm for the Sommer parameter. On both configuration sets we found $r_0/a = 4.25(2)$ (the error is from the larger volume set where we have a better signal for the potential), giving $a = 0.1153(5)$ fm. With this value the physical volumes are $(1.85 \text{ fm})^4$ and $(2.77 \text{ fm})^4$. Based on the PCAC quark mass and the pseudoscalar and axialvector renormalization factors (see Sec. III), we estimate the renormalized quark mass in the $\overline{\text{MS}}$ scheme at 2 GeV to be 22 and 8.5 MeV, respectively. These values, and some other details of the simulation, are listed in Table I.

The dynamical simulations were performed at particularly low quark masses, even if we

κ	κ_{rew}	L	N_{conf}	$a m_{\text{PCAC}}$	$m[\text{MeV}]$
0.1278	0.1278	16	180	0.0117(3)	22
	0.1279	16	180	0.0088(5)	16.5
	0.1280	16	180	0.0058(7)	11
	0.12805	16	180	0.0047(8)	9
	0.1281	16	180	0.0028(11)	5
0.12805	0.12805	24	154	0.0044(3)	8.5
	0.12810	24	154	0.0030(3)	5.8
	0.128125	24	154	0.0024(3)	4.2
	0.12815	24	154	0.0019(4)	3.8

Table I: The parameters of the simulation. The first column gives the coupling κ of the dynamical simulation, the second the reweighted coupling κ_{rew} . The last column is the renormalized quark mass using $m = m_{\text{PCAC}}Z_A/Z_P$.

consider the relatively large volumes. This is possible due to the highly improved chiral properties of the nHYP smeared clover fermions. Figure 1 shows the histogram of the absolute value of the lowest Hermitian eigenmode of the configurations. Simulations with Wilson-like fermions require a well defined gap between zero and the first eigenmode [18]. As the figure shows, our simulations are safe on both volumes, though very close to the low mass limit. In both cases, the median of the distribution is about four times its width σ , which is above the 3σ stability criterion of Ref. [18]. However, it also shows that going lower in the quark mass can be very dangerous because of the algorithm becoming unstable. The same paper predicts $\sqrt{V}\sigma/a$ to be a scaling quantity. We measure 0.56(4) and 0.77(5) for the 24^4 and 16^4 ensembles respectively.

Starting from the original configurations one can explore a range of quark masses in fully dynamical systems by reweighting the configurations. In Ref. [5] we have described an effective technique to calculate the necessary weight factors. It is a stochastic calculation, and one must take care not to introduce significant statistical errors with the stochastic process. We apply three methods, low mode separation, determinant breakup, and ultraviolet (UV) noise reduction to control the statistical fluctuations. In both the 16^4 and 24^4 ensembles we separate 6 low Hermitian eigenmodes. In addition we break up the determinant to the product of 33 and 60 terms for each $\Delta\kappa = 0.0001$ shift in reweighting on the 16^4 and 24^4 volumes, respectively. To control and remove some of the UV noise we introduce a pure gauge term in the reweighted action. This term is just an nHYP plaquette term and has a very small coefficient. We found that in our system it can be chosen to be proportional to the shift in κ ,

$$\beta_{\text{nHYP}} = 6.0(\kappa - \kappa_{\text{rew}}) \quad (1)$$

on both the 16^4 and 24^4 configuration sets. This value is so small that there is no difference within the errors in the lattice spacings or quark masses between $\beta_{\text{nHYP}} = 0$ and Equation 1. For further details and the exact definition of the reweighting action we refer to Ref. [5],

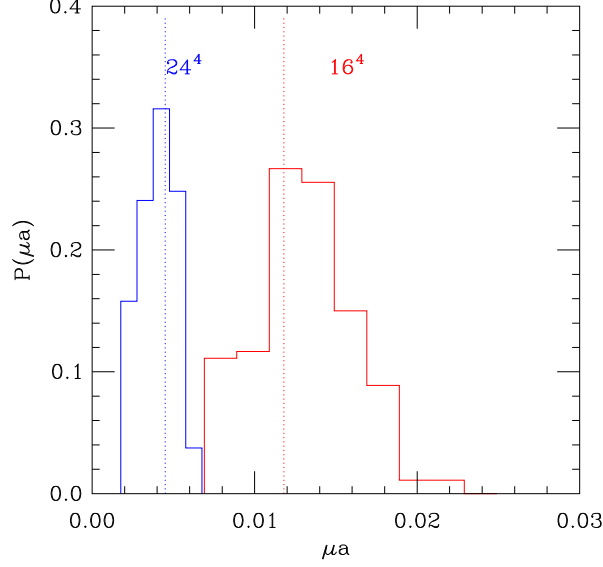


Figure 1: The Hermitian gap distribution on the original 16^4 and 24^4 configurations. The dashed lines correspond to am_{PCAC} .

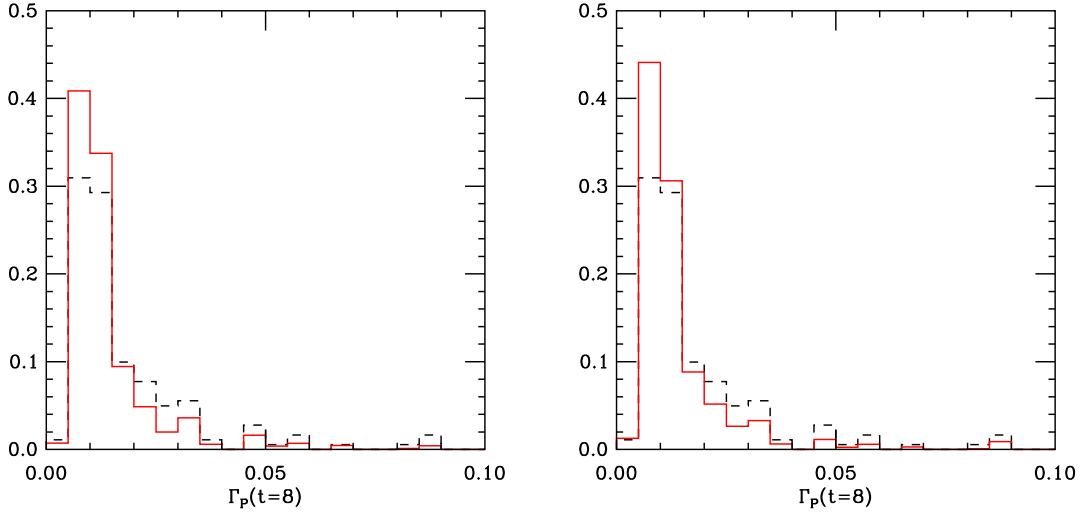


Figure 2: The distribution of the pseudoscalar correlator at $t = 8$ on the 16^4 ensemble at $\kappa = 0.1280$. On both panels the dashed line is the partially quenched distribution and the solid lines correspond to the reweighted distributions. Left panel: $\beta_{nHYP} = 0$, right panel: β_{nHYP} as in Equation 1.

especially Equation 17 and Figure 4.

In addition to removing the UV fluctuations, the introduction of the nHYP plaquette term also increases the overlap between the original and target ensembles. The largest weight factors are pushed from the edge of the plaquette distribution to the middle, where the statistical sampling is better, and the effect is similar for other observables as well. We illustrate this in Figure 2 with the distribution of the pseudoscalar correlator at $t = 8$. All data correspond to the 16^4 data set at $\kappa = 0.1280$. The left panel shows the reweighted

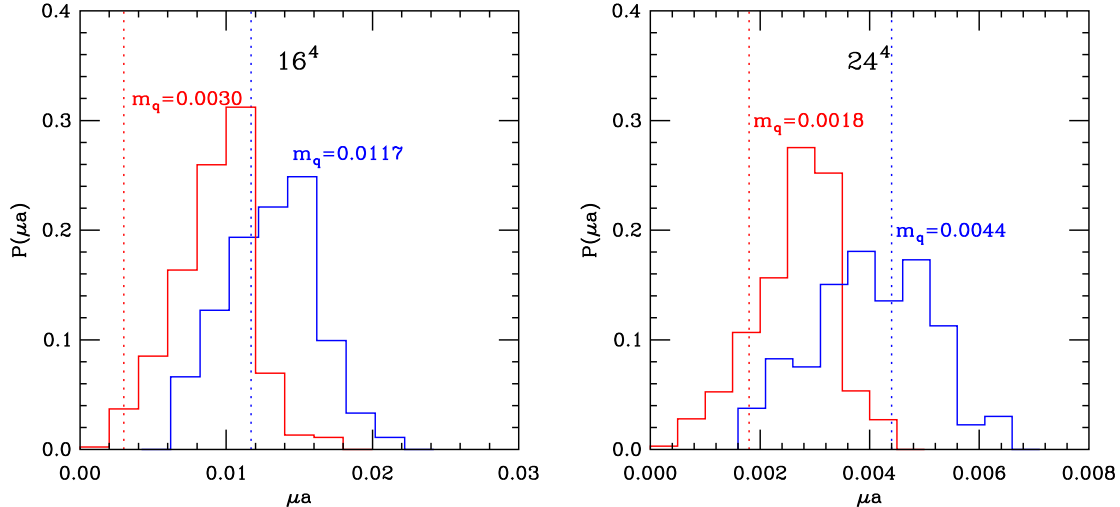


Figure 3: The Hermitian gap distribution on the original and lightest reweighted ensembles for both volumes. The histograms are labeled by the corresponding lattice quark mass which is also indicated by the dashed lines.

distribution without the nHYP plaquette term, the right one with β_{nHYP} as in Equation 1. For reference both panels show the partially quenched (unweighted) distribution. In both cases the overlap between the reweighted and partially quenched distributions is excellent, there is no sign that reweighting would prefer region that is poorly sampled by the original ensemble. The main difference between the reweighted and partially quenched data is the suppression of the long tail of the latter one, a quenching artifact. The apparent increase of the reweighted distributions is mainly due to normalization: the dynamical distribution is narrower, resulting in a higher peak. It is worthwhile to emphasize that including the nHYP plaquette term does not introduce any systematic error, rather it improves the overlap between the ensembles, especially at larger mass difference.

Even though there is no strong difference between the two panels of Figure 2, the introduction of the nHYP plaquette term reduces the statistical errors by up to 40% for our lightest 16^4 data set, and the results we present in the following reflect that. On the other hand, on the 24^4 volumes within the κ range we reweight to there is no difference between the actions with or without the nHYP plaquette term, and the results we present here were obtained with $\beta_{\text{nHYP}} = 0$.

With reweighting it is possible to reach an eigenvalue that is negative or at least smaller than the typical eigenvalues of the Dirac operator. We approach that case with our last coupling on the 16^4 ensemble where at least one configurations has a negative real Dirac eigenvalue and several has nearly zero eigenvalues, and even more on the lightest reweighted 24^4 configurations where 5% of the configurations have a negative Dirac eigenvalue and even more have a nearly zero one. These configurations are suppressed by the weight factor, nevertheless as we will see later one encounters increased statistical errors on these ensembles. In Figure 3 we compare the Hermitian gap distribution on the original and lightest reweighted ensembles for both volumes. The distribution shifts towards zero but configurations with

negative or near-zero eigenmodes are strongly suppressed, and that maintains the gap. While the PCAC quark mass approaches zero, the median of the gap, controlled by the finite volume, remains finite.

III. RENORMALIZATION FACTORS

In order to connect the lattice meson correlators to the physical ones we have to determine the corresponding renormalization factors. We used the standard RI-MOM method [19], where one calculates bilinear quark operators $\langle p|O_{\Gamma}|p\rangle$ at specific lattice momentum $p^2 = \mu^2$ and matches them to the corresponding tree-level matrix element. Afterwards the lattice values are connected to the continuum $\overline{\text{MS}}$ scheme perturbatively [20, 21]. The renormalization scale μ has to be much smaller than the lattice cut-off to minimize lattice artifacts but much larger than the QCD scale for continuum perturbation theory to work.

Our code to calculate the lattice matrix elements is based on the one used in Ref. [22]. We used 80 propagators from the 16^4 data set to calculate the vector, axialvector, scalar and pseudoscalar matching factors in the chiral limit. While most dynamical calculations do the chiral extrapolations on partial quenched data [23],[24], we can do this extrapolation on fully dynamical configurations on our reweighted ensembles. We used 5 κ values, 0.1278, 0.12785, 0.1279, 0.12795 and 0.1280, corresponding to quark masses 10-20 MeV. We extrapolated the vector, axial and scalar data linearly in the quark mass, though the data shows no mass dependence within errors. This is not that surprising, since our quark masses are light. The pseudoscalar density couples to the Goldstone boson channel and it develops an $\mathcal{O}(1/m)$ singularity in the chiral limit. We subtract this pole assuming a linear mass dependence for the quantity m/Z_P . Again, with our light mass values we expect this assumption to hold, and our data are indeed consistent with a linear dependence [25, 26]. Nevertheless the subtraction introduces fairly large errors at small μ .

In Figure 4 we show all four renormalization factors converted to the $\overline{\text{MS}}$ scheme at 2GeV, as the function of the original lattice momentum $p^2 = \mu^2$. The vector and axialvector factors are scale independent, any deviation from a constant is due to lattice artifacts. In our case Z_V is constant over the whole range, while Z_A shows a slight drift at larger μ values. Calculations with Wilson and Wilson-like improved fermions show similar trends for these quantities [23, 25, 26].

The scalar and pseudoscalar operators depend on the energy scale. We connect the lattice data to the continuum one at identical energy, then, using the known 3-loop expression for the running of the coupling, run it to $\mu = 2\text{GeV}$. We plot these values, therefore Z_P and Z_S in Figure 4 should also be constant. Because of the subtraction of the Goldstone pole the errors are large at small μ for the pseudoscalar, but we find a long, stable plateau at larger lattice scale values. The scalar operator, on the other hand, shows quite large lattice artifacts at higher scales. Again, this trend has been observed before with other actions. The horizontal lines in Figure 4 indicate the range where we extract the renormalization

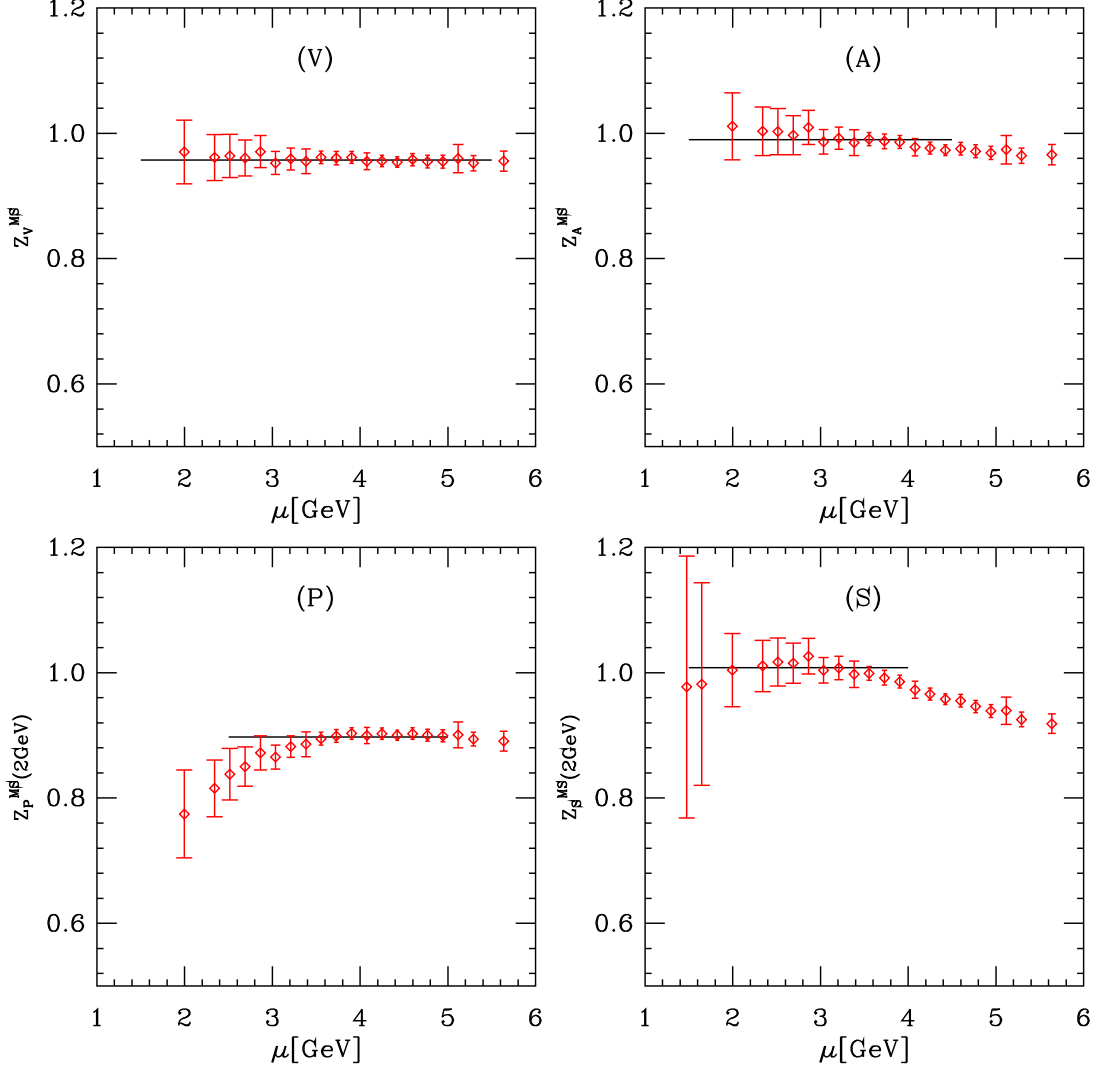


Figure 4: The renormalization factors for the vector, axialvector, pseudoscalar and scalar operators as the function of the lattice energy scale. All values are converted to the continuum $\overline{\text{MS}}$ scheme at $\mu = 2\text{GeV}$.

factors. Our final values are

$$\begin{aligned}
 Z_V^{\overline{\text{MS}}} &= 0.96(1) \\
 Z_A^{\overline{\text{MS}}} &= 0.99(2) \\
 Z_P^{\overline{\text{MS}}}(2\text{GeV}) &= 0.90(2) \\
 Z_S^{\overline{\text{MS}}}(2\text{GeV}) &= 1.01(3).
 \end{aligned} \tag{2}$$

As a simple check we compare the renormalized quark mass as predicted from the bare quark mass $m = Z_S^{-1}m_b$, $1/(2\kappa) - 1/(2\kappa_{cr})$, and from the PCAC mass $m_r = Z_A Z_P^{-1}m_{\text{PCAC}}$. Fitting m_{PCAC} linearly in $1/(2\kappa)$ we predict $\kappa_{cr} = 0.12821$ and from the slope $Z_P Z_S^{-1} Z_A^{-1} = 0.94(3)$. This is consistent from the value obtained from Equation 2, 0.90(7). The fact that all four matching factors are close to one indicates small perturbative corrections, as it is usually

seen with smeared link actions.

IV. ϵ -REGIME ANALYSIS

In the ϵ -regime the pion correlation length is large compared to the linear size of the lattice, the light pseudoscalar mesons dominate the dynamics. Nevertheless, in order to incorporate the massive modes the volume has to be large compared to the QCD scale. One assumes that the quark mass is $m = \mathcal{O}(\epsilon^4)$ and the inverse size $1/L = \mathcal{O}(\epsilon)$ ($L^4 = V = L_s^3 L_t$), but $1/L \gg \Lambda_{\text{QCD}}$. The dimensionless quantity $m\Sigma V$, or equivalently $m_\pi^2 F_\pi^2 V$, is kept order one. Chiral perturbation theory predictions are organized in power of ϵ^2 or $1/(FL)^2$. Predictions for various meson correlators are known to next-to-leading (NLO) order ($\mathcal{O}(\epsilon^4)$), except for the pseudoscalar that has been calculated up to $\mathcal{O}(\epsilon^6)$. In our fits we use the NLO predictions as those depends only on two low-energy constants, $\Sigma = \lim_{m \rightarrow 0} \langle \bar{q}q \rangle$ and $F = \lim_{m \rightarrow 0} F_\pi$ [3, 4, 27]. These χ PT results are based on a chiral (continuum) action. One expects extra terms, due to the explicit chiral symmetry violation of the Wilson fermion action, in our situation. However these corrections typically show up at the same order as the higher order chiral constants L_3, L_4 , i.e. only at next-to-next-to-leading order in the epsilon regime.

As the quark mass decreases in a large volume (p-regime) simulation, the chiral symmetry breaking effects of Wilson fermions get large compared to the mass, and that can create large lattice artifacts. In practice the continuum limit has to be taken before the chiral limit. The situation is different in the ϵ -regime, where the finite volume of the system creates an infrared cutoff even at vanishing quark mass. This effect is well illustrated by the Hermitian gap distribution in Figure 3. While in infinite volume one expects the median of the gap to scale with the mass $\bar{\mu} = Z_A m_{\text{PCAC}}$ [28], in the ϵ -regime $\bar{\mu}$, governed by the IR cutoff of the volume, remains finite while $m_{\text{PCAC}} \rightarrow 0$. This is clearly the case in our simulations. Therefore one does not need a chiral action to study the epsilon regime, though the explicit symmetry breaking effects should be small compared to the inverse lattice size. As long as the volume is large enough that the NLO relations describe the two-point functions, continuum χ PT results can be used to analyze Wilson fermion data. Since separating topological sectors with Wilson fermions is not always possible, we analyze our data averaged over the topological charge.

For completeness we give the relevant formulas for two degenerate flavors, averaged over the topological charge. The isotriplet pseudoscalar meson correlator up to $\mathcal{O}(\epsilon^4)$ is

$$\begin{aligned} \Gamma_P(t) &= \frac{1}{L_s^3} \int d^3x \langle P(x)P(0) \rangle \\ &= \Sigma^2 \left(a_p + \frac{L_t}{F^2 L_s^3} b_p h_1\left(\frac{t}{L_t}\right) + \mathcal{O}(\epsilon^4) \right), \end{aligned} \quad (3)$$

where $P(x, t) = \bar{\psi} \frac{1}{2} \lambda^i \gamma_5 \psi$ is the pseudoscalar density operator and

$$a_p = \frac{\rho}{8} I_1(u). \quad (4)$$

$$b_p = 1 - \frac{1}{8}I_1(u),$$

with

$$\rho = 1 + \frac{3\beta_1}{2(FL)^2}$$

the shape factor ($\beta_1 = 0.14046$ for our symmetric geometry) and

$$u = 2m\Sigma V \rho.$$

I_1 can be expressed in terms of Bessel functions, $I_1(u) = 8Y'(u)/(uY(u))$. It decreases smoothly from 2 at $u = 0$ to 0.68 at $u = 10$, the largest value we encounter. The function

$$h_1(\tau) = \frac{1}{2}\left[\left(\tau - \frac{1}{2}\right)^2 - \frac{1}{12}\right] \quad (5)$$

describes the quadratic time dependence. The pseudoscalar correlator is dominated by Σ , the dependence on F is only through the $\mathcal{O}(\epsilon^2)$ term.

The flavor triplet axialvector current correlator at NLO is

$$\begin{aligned} \Gamma_A(t) &= \frac{1}{L_s^3} \int d^3x \langle A_0(x) A_0(0) \rangle \\ &= \frac{F^2}{V} \left(a_a + \frac{L_t}{F^2 L_s^3} b_a h_1\left(\frac{t}{L_t}\right) + \mathcal{O}(\epsilon^4) \right), \end{aligned} \quad (6)$$

with $A_0(x, t) = \bar{\psi} \frac{1}{2} \lambda^i \gamma_0 \gamma_5 \psi$ and

$$\begin{aligned} a_a &= 1 - \frac{1}{4}I_1(u) + \frac{\beta_1}{(FL)^2} \left(2 - \frac{1}{2}I_1(u) \right) - \frac{L_t}{F^2 L_s^3} \frac{k_{00}}{2} I_1(u), \\ b_a &= \frac{1}{8}u^2 I_1(u). \end{aligned} \quad (7)$$

In our $L_s = L_t$ case $k_{00} = \beta_1/2$. The axialvector correlator is dominated by F , the dependence on Σ enters only through the combination $m\Sigma V$.

The ϵ -expansion formulas are systematic expansions in the parameter $1/(FL)^2 = \mathcal{O}(\epsilon^2)$, but depend on the $\mathcal{O}(1)$ quantity $m\Sigma V$. In our simulation we explore the range $m\Sigma V \approx 0.7 - 5.0$. Large values introduce large NLO and NNLO corrections to the correlators, and at some point one transitions into the large volume p -regime. Only by examining the fit results will we be able to decide what range of $m\Sigma V$ values are acceptable in the ϵ -regime.

The lattice correlators have to be multiplied by the renormalization factors Z_P^2 and Z_A^2 to obtain the continuum ones in Equations 3 and 6, while in the product $m\Sigma V$ the quark mass can be expressed in terms of the PCAC mass as $m = m_{\text{PCAC}} Z_A/Z_P$. In our fit we use the combinations

$$\Gamma_A = Z_A^2 \Gamma_A^{(\text{latt})} \quad (8)$$

and

$$m^2 \Gamma_P = Z_A^2 m_{\text{PCAC}}^2 \Gamma_P^{(\text{latt})} \quad (9)$$

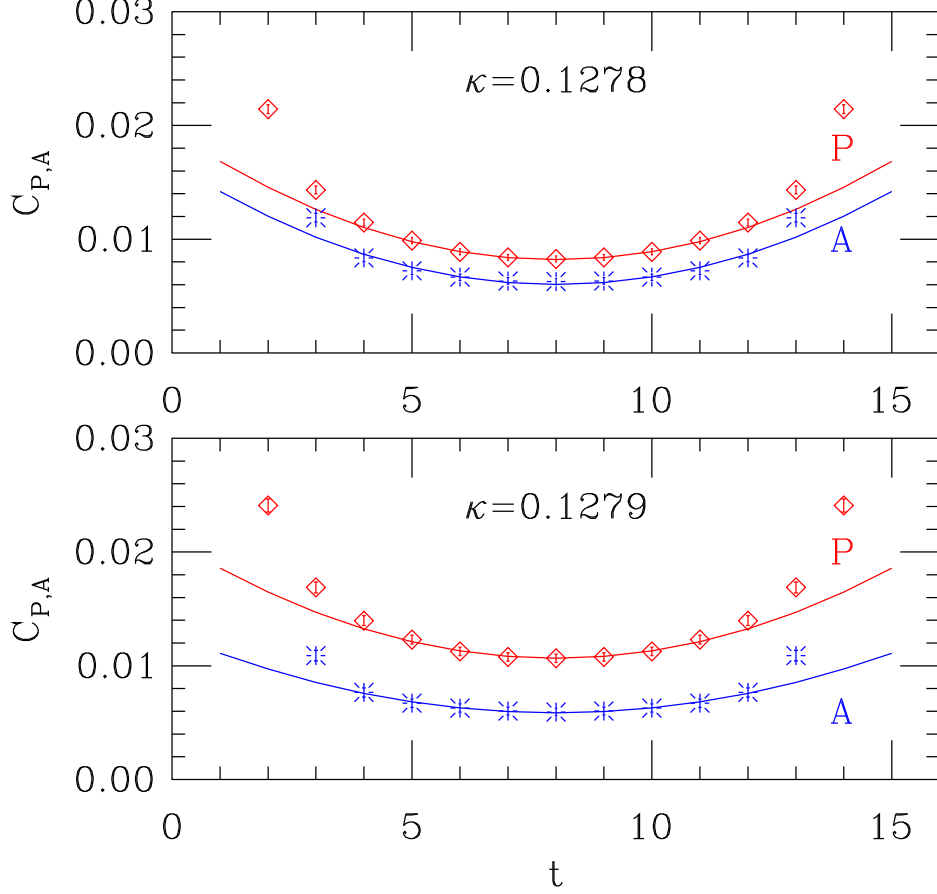


Figure 5: The pseudoscalar (red diamonds) and axialvector (blue bursts) lattice correlators and the combined fit results at $\kappa = 0.1278$ and 0.1279 on the 16^4 data set. The axialvector correlators are multiplied by the factor 50 to better match the scale of the pseudoscalar.

that depend only on F and $m\Sigma V$, and do a combined fit to Equations 8 and 9.

The results of the combined fits on the 16^4 lattices are shown in Figures 5 and 6, where we plot both the pseudoscalar and axialvector correlators (the latter is rescaled by a factor 50 to match the scale). We use the time slices $[5, 11]$ in the fit. The data are well described by the NLO formulas at all four mass values. The results are summarized in Table II where we list not only the predicted low-energy parameters but the combination $m\Sigma V$ and an estimate for $m_\pi L$ as well. We estimate the infinite volume pion mass using the GMOR relation $m_\pi^2 = N_f m \Sigma / F^2 + \mathcal{O}(m^2)$. In the ϵ -regime one requires $m_\pi L \ll 1$, though according to the analysis of Ref. [4], the ϵ - and p -regimes connect smoothly around $m_\pi L \approx 2$, so values up to that level are also acceptable. While at $\kappa = 0.1278$ both $m\Sigma V$ and $m_\pi L$ are somewhat large, the fit indicates that the data are described well by the ϵ -regime forms at all κ values. The predicted low-energy constants, especially F , show a slight drift as m decreases, indicating that higher order effects are nevertheless not negligible. Considering that the expansion parameter $1/(FL)^2 \approx 1.45$ is not at all small, this is quite possible. The $\mathcal{O}(\epsilon^2)$ corrections to the pseudoscalar correlator at $t = N_t/2$ in Equation 4 are 34% at $\kappa = 0.1278$, decreasing to 16% at $\kappa = 0.1281$, while the constant term a_a of the axial correlator in Equation 7 has

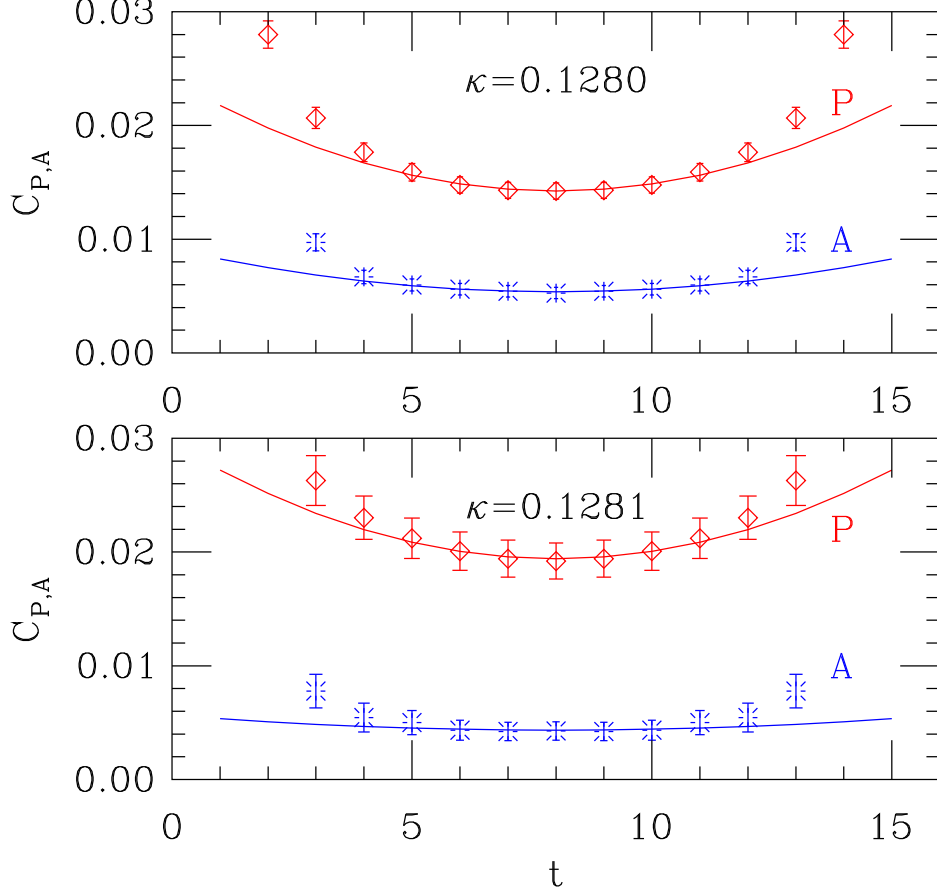


Figure 6: Same as Figure 5 but at $\kappa = 0.1280$ and 0.1281 .

30-25% corrections in the same range. A volume of $(1.85\text{fm})^4$ is not large enough to suppress finite volume effects.

Our second data set is 24^4 , $(2.77\text{fm})^4$, considerably larger. The $\mathcal{O}(\epsilon^2)$ corrections are reduced to $\approx 15\%$ for the axial correlator, though the corrections are still large, 10-25% for the pseudoscalar correlator at our mass values. Figures 7 and 8 show the result of the combined fit. Again, we find good agreement for all correlators in the range of $5 \leq t \leq 19$, though we use only time slices $[8, 16]$ in the fit. The statistical errors are under control everywhere, though they increase as the reweighting range increases .

The data points for $t < 5$ and $t > L_t/a - 5$ do not follow the ϵ -regime χ PT predictions. A natural explanation is that the heavy excitations that couple to the operators die out only at $t \geq 5$ and influence the correlators at small distances. If that is indeed the case, the correlators should show similar behavior on the 16^4 and 24^4 sets. Indeed, at $\kappa = 0.12805$ and $\kappa = 0.1281$, where we have results on both volumes, both the pseudoscalar and axialvector correlators are identical within errors for $t < 5$, showing the same transient behavior. It is somewhat puzzling why a recent result using overlap fermions at similar lattice spacing and even smaller quark masses see transient behavior in the pseudoscalar channel up to $t \approx 12$ [14]. It might be due to the small spatial extent ($L_s = 16$) or the asymmetric geometry ($L_t = 32$) used in Ref. [14], or that the overlap operator is more extended and excited states

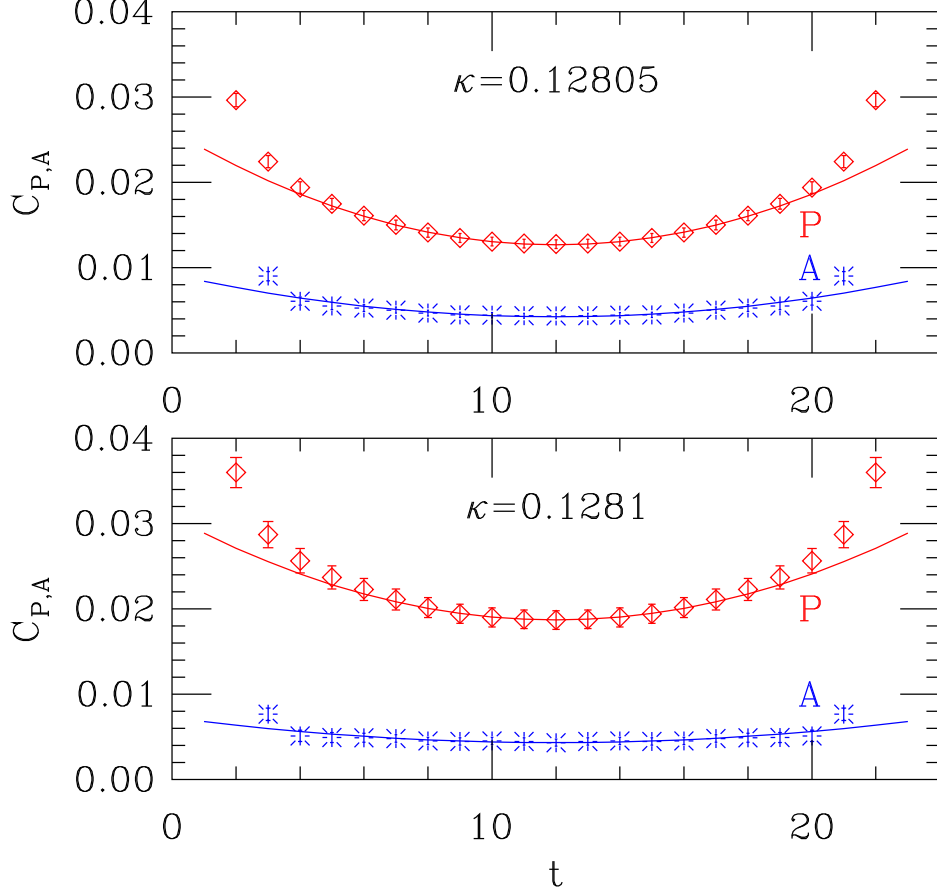


Figure 7: Same as Figure 5 but on the 24^4 data set at $\kappa = 0.12805$ and 0.1281 .

κ	L	$m\Sigma V$	$m_\pi L$	$F[\text{MeV}]$	$\Sigma^{1/3}[\text{MeV}]$
0.1278	16	3.1(2)	3.14	90(3)	256(6)
0.1279	16	2.1(1)	2.58	86(4)	254(6)
0.1280	16	1.4(1)	2.11	83(6)	252(7)
0.12805	16	1.0(1)	1.78	82(7)	250(7)
0.1281	16	0.68(5)	1.47	76(10)	251(7)
0.12805	24	5.2(3)	2.71	90(3)	248(6)
0.12810	24	3.4(2)	2.19	89(4)	250(6)
0.128125	24	2.6(1)	1.91	89(6)	248(6)
0.12815	24	2.3(1)	1.80	92(8)	245(8)

Table II: Results from the combined fit to the pseudoscalar and axialvector correlators. The values of F and Σ are converted to physical units using $r_0 = 0.49\text{fm}$. The combination $m\Sigma V$ is predicted by the fit while for $m_\pi L$ we estimate the infinite volume pion mass from the GMOR relation.

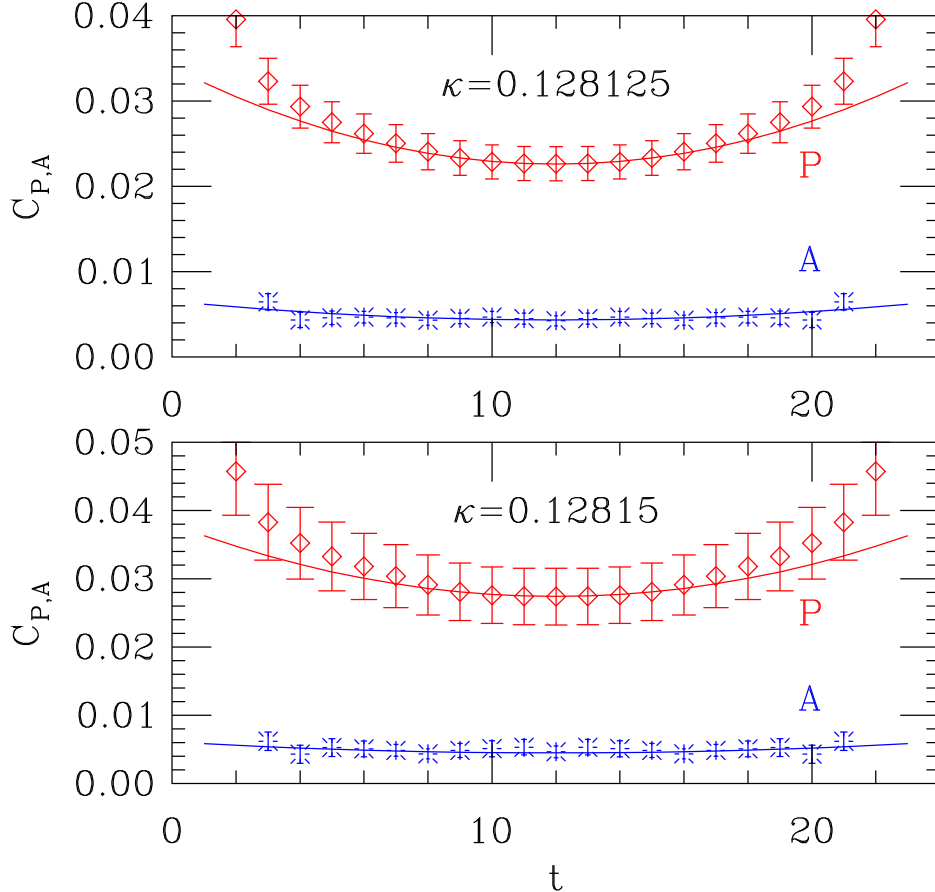


Figure 8: Same as Figure 5 but on the 24^4 data set at $\kappa = 0.128125$ and 0.12815 .

die out slower.

We also have measurements of the vector current correlator. The data and the fit quality are similar to the axialvector we presented above. Since it does not improve the determination of the low-energy constants, we do not include it in our analysis.

One might ask if the data, especially on the 16^4 volumes, could be better fitted with NNLO, $\mathcal{O}(\epsilon^6)$ forms. For the pseudoscalar these two-loop results are known in the continuum [27], and contain two new low-energy constants, L_3 and L_4 . On the lattice additional terms, due to the chiral symmetry breaking of the Wilson action, also enter. For the axialvector correlator only NLO results are available. Considering the number of unknown parameters, it is not obvious that a meaningful fit could be done even if full NNLO formulas were available, though it would be very interesting to test.

We close this section with a combined plot of the low-energy constants obtained on the two volumes, as the function of the parameter $m\Sigma V$ (Figure 9).

As is evident both from Figure 9 and Table II, the different quark mass data on the 24^4 ensemble are consistent for both low-energy constants and the results for the chiral condensate are consistent on the two volumes. F , on the other hand, shows a drift as $m\Sigma V$ decreases. Without a large volume data point at $m\Sigma V < 2$ we cannot tell if this is due to finite volume effects, or signals the breakdown of the ϵ expansion for $m\Sigma V > 2$. χ PT

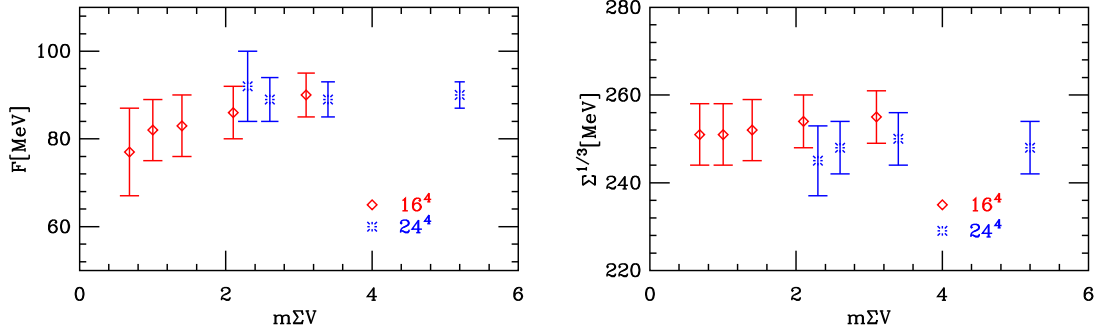


Figure 9: The low-energy constant F and $\Sigma^{1/3}$ as the function of the parameter $m\Sigma V$, predicted by NLO χ PPT.

formulas that connect the ϵ and p regimes could help to decide this issue. Since the next-to-leading order corrections to F are over 10% on the 16^4 data set, we prefer using the large volume data to arrive at our final prediction,

$$\begin{aligned}
 F &= 90(4)\text{MeV}, & \Sigma^{1/3} &= 248(6)\text{MeV} \\
 Fr_0 &= 0.224(10), & \Sigma^{1/3}r_0 &= 0.617(15).
 \end{aligned}
 \tag{10}$$

The errors only include the statistical uncertainties.

Let us finally compare our results to other recent two flavor computations, even though direct comparisons are problematic due to different systematic errors. In the p -regime with maximally twisted mass fermions, the ETM collaboration gets in the continuum limit $Fr_0 = 0.188(2)(7)$ and $\Sigma^{1/3}r_0 = 0.597(9)(15)$ and a compatible number for Σ in the ϵ regime [15, 29]¹. Another ϵ regime computation has been performed by JLQCD with dynamical overlap fermions at fixed topology in a $L^3 \times 2L$, $L = 1.8\text{fm}$ box [14]. They get $Fr_0 = 0.217(14)$ and $\Sigma^{1/3}r_0 = 0.596(10)$. Given the statistical and systematic errors, these results nicely agree with our determination.

Another method of extracting the low-energy constant is by looking at the distribution of the lowest eigenvalue of the Dirac operator and comparing it to predictions from random matrix theory. To our knowledge, there are two such results with renormalized $N_f = 2$ results. In Ref. [30], JLQCD compute $r_0\Sigma^{1/3} = 0.624(17)(27)$ using these methods. Ref. [31] finds $r_0F = 0.213(11)$ and $r_0\Sigma^{1/3} = 0.594(13)$ using nHYP link dynamical overlap fermions. Again, there is good agreement to our findings.

V. CONCLUSION

The data presented in this paper has been generated with moderate computer resources. This was possible due to the good chiral properties of the action which come at relatively low cost due to the simple nHYP smearing procedure, and the effective reweighting that

¹ The number for Σ is not explicitly given; the quoted errors are obtained using $r_0 = 0.433\text{fm}$

allowed us to lower the quark mass even further. Obviously, there are still shortcomings of our analysis. The simulation is done at just one lattice spacing, so we are not able to take our results to the continuum limit. However, HYP smearing has improved the scaling properties of a variety of actions. We are confident that also here cut-off effects will be small.

Moreover, setting the scale by $r_0 = 0.49\text{fm}$ is not satisfactory. The value of r_0 is not known to high accuracy. We could use F as scale parameter. Apart from that, the ϵ regime setup makes it problematic to use other widely used scales like the mass of the Ω baryon.

We still are at finite lattice size and ϵ -regime χ PT is a slowly converging expansion in $1/(FL)^2$. Here, our large volume puts us into a good position and the comparison between the $L/a = 16$ and $L/a = 24$ results shows that the finite volume effects are under control. However, statistical errors due to the limited number of gauge configurations are too large for a more substantiated claim.

For the ϵ expansion to be valid, the parameter $m\Sigma V$ has to be $\mathcal{O}(1)$. Our data span the range 0.7 to 5.2 and might go beyond the validity of the analytical expressions. An expansion that connects the ϵ and p regimes would be very useful to control this aspect of the calculation.

Nevertheless our results are encouraging. We find that reweighting works on a fairly large volume of $(L/a)^4 = 24^4$, $L \approx 2.8\text{fm}$, and the statistical fluctuations are under control despite quark masses as low as 4MeV. Repeating the calculation at a smaller lattice spacing would not be prohibitively expensive and could improve on all of the above mentioned issues.

VI. ACKNOWLEDGEMENT

We have benefited from discussion with O. Bär, G. Colangelo, T. DeGrand, P. Hasenfratz, T. Izubuchi, S. Necco, and F. Niedermayer. Most of the numerical work reported in this paper was carried out at the kaon cluster at FNAL. We acknowledge the support of the USQCD/SciDac collaboration.

The renormalization constants calculation was done based on the code developed by T. DeGrand and Z-f. Liu. We are grateful for the permission to use it. This research was partially supported by the US Department of Energy and the Deutsche Forschungsgemeinschaft in the SFB/TR 09.

-
- [1] J. Gasser and H. Leutwyler, Ann. Phys. **158**, 142 (1984).
 - [2] J. Gasser and H. Leutwyler, Phys. Lett. **B188**, 477 (1987).
 - [3] F. C. Hansen, Nucl. Phys. **B345**, 685 (1990).
 - [4] F. C. Hansen and H. Leutwyler, Nucl. Phys. **B350**, 201 (1991).
 - [5] A. Hasenfratz, R. Hoffmann, and S. Schaefer (2008), 0805.2369.
 - [6] A. Hasenfratz, R. Hoffmann, and S. Schaefer, JHEP **05**, 029 (2007), hep-lat/0702028.
 - [7] S. Schaefer, A. Hasenfratz, and R. Hoffmann, PoS **LATTICE2007**, 132 (2006), 0709.4130.

- [8] W. Bietenholz, T. Chiarappa, K. Jansen, K. I. Nagai, and S. Shcheredin, JHEP **02**, 023 (2004), hep-lat/0311012.
- [9] L. Giusti, P. Hernandez, M. Laine, P. Weisz, and H. Wittig, JHEP **01**, 003 (2004), hep-lat/0312012.
- [10] L. Giusti, P. Hernandez, M. Laine, P. Weisz, and H. Wittig, JHEP **04**, 013 (2004), hep-lat/0402002.
- [11] H. Fukaya, S. Hashimoto, and K. Ogawa, Prog. Theor. Phys. **114**, 451 (2005), hep-lat/0504018.
- [12] W. Bietenholz and S. Shcheredin, Nucl. Phys. **B754**, 17 (2006), hep-lat/0605013.
- [13] L. Giusti et al., JHEP **05**, 024 (2008), 0803.2772.
- [14] H. Fukaya et al. (JLQCD) (2007), 0711.4965.
- [15] K. Jansen, A. Nube, A. Shindler, C. Urbach, and U. Wenger, PoS **LATTICE2007**, 084 (2007), 0711.1871.
- [16] S. Necco, PoS **LATTICE2007**, 021 (2006), 0710.2444.
- [17] R. Hoffmann, A. Hasenfratz, and S. Schaefer, PoS **LATTICE2007**, 104 (2007), 0710.0471.
- [18] L. Del Debbio, L. Giusti, M. Lüscher, R. Petronzio, and N. Tantalo, JHEP **02**, 056 (2007), hep-lat/0610059.
- [19] G. Martinelli, C. Pittori, C. T. Sachrajda, M. Testa, and A. Vladikas, Nucl. Phys. **B445**, 81 (1995), hep-lat/9411010.
- [20] V. Gimenez, L. Giusti, F. Rapuano, and M. Talevi, Nucl. Phys. **B531**, 429 (1998), hep-lat/9806006.
- [21] K. G. Chetyrkin and A. Retey, Nucl. Phys. **B583**, 3 (2000), hep-ph/9910332.
- [22] T. A. DeGrand and Z.-f. Liu, Phys. Rev. **D72**, 054508 (2005), hep-lat/0507017.
- [23] D. Becirevic et al., Nucl. Phys. **B734**, 138 (2006), hep-lat/0510014.
- [24] P. Dimopoulos et al., PoS **LATTICE2007**, 241 (2006), 0710.0975.
- [25] D. Becirevic et al., JHEP **08**, 022 (2004), hep-lat/0401033.
- [26] C. Gattringer, M. Göckeler, P. Huber, and C. B. Lang, Nucl. Phys. **B694**, 170 (2004), hep-lat/0404006.
- [27] P. Hasenfratz and H. Leutwyler, Nucl. Phys. **B343**, 241 (1990).
- [28] L. Del Debbio, L. Giusti, M. Lüscher, R. Petronzio, and N. Tantalo, JHEP **02**, 011 (2006), hep-lat/0512021.
- [29] P. Dimopoulos, R. Frezzotti, G. Herdoiza, C. Urbach, and U. Wenger (ETM), PoS **LATTICE2007**, 102 (2007), 0710.2498.
- [30] H. Fukaya et al., Phys. Rev. **D76**, 054503 (2007), 0705.3322.
- [31] T. DeGrand and S. Schaefer, Phys. Rev. **D76**, 094509 (2007), 0708.1731.